Drug Design, Development and Therapy

Dovepress

open access to scientific and medical research

Open Access Full Text Article

ORIGINAL RESEARCH

Integrated Microbiome and Metabolome Analysis Reveals Correlations Between Gut Microbiota Components and Metabolic Profiles in Mice with Methotrexate-Induced Hepatoxicity

Changshui Wang[1,*], Shuzhen Zhao[2,*], Yuan Xu[3], Wenxue Sun[4], Yuanyuan Feng[2], Deshuai Liang[5], Yun Guan[3]

[1]Department of Neurosurgery, Affiliated Hospital of Jining Medical University, Jining Medical University, Jining, 272000, People's Republic of China; [2]Children's Rehabilitation Center, Jining Maternal and Child Health Family Planning Service Center, Jining, 272000, People's Republic of China; [3]Department of Hematology, Jining NO. 1 People's Hospital, Jining, 272000, People's Republic of China; [4]Institute of Clinical Pharmacy and Pharmacology, Jining NO. 1 People's Hospital, Jining Medical University, Jining, 272000, People's Republic of China; [5]Department of pharmacy, Jining NO. 1 People's Hospital, Jining, 272000, People's Republic of China

*These authors contributed equally to this work

Correspondence: Yun Guan; Deshuai Liang, Jining NO. 1 People's Hospital, 6 Jiankang Road, Jining, Shandong, 272000, People's Republic of China, Tel/Fax +86-0537 2087092, Email gyuanun1989@163.com; 13468322037@163.com

Purpose: We designed this study to investigate the potential correlations between gut microbiota compositions and hepatic metabolomic disorders in mice with methotrexate (MTX)-induced hepatoxicity.

Methods: We used MTX to induce hepatoxicity in healthy Kunming mice, and we determined plasma ALT and AST levels and assessed the liver tissue histopathology. We applied an integrated gas chromatography-mass spectrometry (GC-MS) and 16S ribosomal RNA (rRNA) gene sequencing approach to evaluate the effects of MTX on the gut microbiota and hepatic metabolic profiles of mice. We uncovered correlations between the gut microbiota and hepatic metabolomic profiles by calculating the Spearman correlation coefficient.

Results: MTX caused ALT and AST level elevations and hepatoxicity in our mouse model. MTX disrupted amino acid metabolic pathways (including biosyntheses of valine, leucine, and isoleucine; and arginine; and, metabolism of alanine, aspartate, and glutamate; histidine; beta-alanine; and glycine, serine, and threonine); biosyntheses of aminoacyl-tRNA; and pantothenate, and CoA; and, metabolic pathways of energy, glutathione, and porphyrin; and chlorophyll. In addition, MTX increased the abundances of *Staphylococcus, Enterococcus, Collinsella, Streptococcus*, and *Aerococcus*, but decreased the amounts of *Lactobacillus, Ruminococcus, norank_f_Muribaculaceae, unclassified_f_Lachnospiraceae, norank_f_Lachnospiraceae, A2, Eubacterium_xylanophilum_group, Phascolarctobacterium, Bifidobacterium*, and *Faecalibaculum*. Our correlation analyses showed that different flora abundance changes including those of *Phascolarctobacterium, Faecalibaculum, norank_f_Muribaculaceae, Streptococcus, Enterococcus, Staphylococcus*, and *Collinsella* were associated with liver injury.

Conclusion: We present evidence supporting the notion that MTX causes hepatoxicity by altering the gut microbiota and hepatic metabolite profiles, our findings provide new venues for the management of MTX-induced hepatoxicity.

Keywords: gas chromatography-mass spectrometry, 16S ribosomal RNA, methotrexate, hepatoxicity

Introduction

Methotrexate (MTX) is an anti-metabolite (folate antagonist) drug used to treat acute leukemia in children and is most frequently used during chemotherapy for various types of cancers (hepatocellular carcinoma, and breast, lung, and gastric cancers).[1] MTX has also been prescribed as an immunosuppressant for auto-immune diseases, such as systemic connective tissue diseases, psoriasis, systemic lupus erythematosus, inflammatory bowel disease, sicca syndrome, and rheumatoid arthritis.[2] Its common

Received: 8 July 2022
Accepted: 2 November 2022
Published: 8 November 2022

adverse effects include gastrointestinal symptoms such as nausea, vomiting, diarrhea, abdominal pain, constipation, pancreatitis, and/or small-bowel obstruction.[3] However, the major adverse effect induced by MTX is hepatotoxicity.[4] Aberrant levels of liver transaminase are commonly observed after receiving MTX, probably accompanied with liver histological alterations. A study on patients with rheumatoid arthritis showed that 15.3% developed mild liver fibrosis, 1.3% severe fibrosis, and 0.5% cirrhosis after MTX administration.[5] However, the underlying mechanisms of MTX-induced hepatotoxicity remain unclarified.

Gut microbiota, also known as "the new virtual metabolic organ", affect the functioning of extraintestinal organs, such as the liver, kidneys, and brain, and that of the cardiovascular and skeletal systems.[6–8] The gut microbiota has been implicated in the pathophysiology of diverse liver diseases.[9] The gut and the liver communicate bi-directionally (gut-liver axis) through the biliary tract, the portal vein, and the systemic circulation. An impaired gut mucosal barrier with increased intestinal permeability facilitates the bacterial translocations into the liver through the gut-liver axis, altering hepatic functions.[10] In addition, the liver interacts with the gut via release of bile acids and bioactive mediators into the biliary tract and the systemic circulation.[10] Differentially-expressed biomarkers in the liver including inosine, taurine, glutathione, aminohydroxybutyric acid, cholic acid, and L-lysine are associated with the gut microbiota abundances, indicating a communication between the hepatic metabolism and the gut microbiota during acute alcohol-induced liver disease.[11] Although MTX-induced liver toxicity has been studied,[12] the association between possible MTX-induced gut microbiota abundance changes and liver damage remains unclear. We hypothesize the existence of an interaction between gut microbiota changes and metabolic hepatic phenotypes induced by MTX administration.

An increasing body of evidence suggests that an integrated metabolomics and 16S rRNA sequencing approach can characterize the gut microbial composition and its association with metabolic phenotypes or functional changes during various diseases.[13,14] In addition, drug-induced toxic or therapeutic effects induced by gut microbiota and metabolism changes can also be elucidated by integrated metabolomics and 16S rRNA sequencing.[15,16] Therefore, we employed an integrated GC-MS-based metabolomics approach with 16S rRNA sequencing to elucidate possible associations between gut microbiota components and hepatic metabolic pathways after MTX exposure. Our results clarify the picture of MTX-induced hepatotoxicity and provide a basis for novel management strategies.

Materials and Methods

Chemicals and Reagents

MTX (purity 99%), heptadecanoic acid (purity ≥ 98%), methanol (chromatographic grade), and pyridine were purchased from Macklin Biochemical (Shanghai, China). O-methylhydroxylamine hydrochloride (purity ≥ 98%) was obtained from J&K Scientific (Beijing, China). N, O-bis(trimethylsilyl) trifluoroacetamide (containing 1% trimethylchlorosilane) was obtained from Sigma Aldrich (St. Louis, MO, USA). Purified water was purchased from Wahaha (Hangzhou, China). All experimental procedures were conducted in compliance with the Guidelines for the Use of Laboratory Animals, and approved by the Ethical Committee for Animal Experimentation of the Affiliated Hospital of Jining Medical University (approval number: 2022B070).

Animals and Treatment

We obtained 14 Kunming mice (age, 5 weeks; weight, 30–35 g) from Pengyue Experimental Animal Breeding (Jinan, China; approval number: SCXK20190003), and we kept them maintained at 20 ± 2 °C with 65% humidity under a 12 h light/dark cycle, with free access to food and water. After 1-week of acclimation, we randomly divided the animals into two groups (seven mice in each group). Mice in MTX group were intraperitoneally injected with MTX (5 mg/kg) every day for 7 days. The dose was adjusted according to the body weight of each mouse (0.1 mL/10 g). Mice in the control group received equivalent amounts of saline. The dose of MTX in this study was chosen on the basis of a previously described protocol[17] with appropriate modifications.

Sample Collection and Preparation

At the end of the MTX challenge period, mice were anesthetized with 1% sodium pentobarbital (50 mg/kg). Blood samples were obtained from each mouse after eyeball enucleation. Serum samples were collected after centrifugation at

4000 rpm for 10 min at 4 °C, and stored at −80 °C until analysis. Animals were sacrificed by cervical dislocation. Immediately thereafter, the liver was excised, frozen in liquid nitrogen, and stored at −80 °C. The colonic contents were also collected into sterile conical tubes, and the colonic lumen was washed with PBS. Finally, the colon was frozen in liquid nitrogen and stored at −80 °C.

We homogenized 50 mg of liver sample with 1 mL of methanol, and then mixed the paste with 50 μL of heptadecanoic acid (1 mg/mL in methanol). After centrifugation at 4 °C for 15 min at 14,000 rpm, we added 80 μL of O-methylhydroxylamine hydrochloride (15 mg/mL in pyridine) at 70 °C for 90 min, followed by addition of 100 μL of N, O-bis(trimethylsilyl) trifluoroacetamide (containing 1% trimethyl chlorosilane) at 70 °C for 60 min. We used the N, O-bis(trimethylsilyl) trifluoroacetamide (99% BSTFA+1% TMCS) for derivatization and the heptadecanoic acid (1 mg/mL) as an internal standard. We purified the samples through a 0.22-μm filter. Finally, we pooled together 10 μL of each sample in a group (control or MTX groups) as quality controls (QC).

Hepatoxicity Indicator Determination

Alanine aminotransferase (ALT) and aspartate aminotransferase (AST) assay kits were purchased from Jiancheng Bioengineering Institute (Nanjing, China). We measured serum ALT and AST levels with a spectrophotometer following the manufacturer's protocols (UNICO Instruments, Model 1200, USA).

Histopathological Examination

The liver samples for the histopathological examination were dehydrated with ethanol and xylene, embedded in paraffin, sectioned at a 5 μM thickness, and stained with Hematoxylin and Eosin (H&E). We scanned the stained liver sections with a 3D panoramic scanner (HISTECH Panoramic 250, Hungary) and identified the fields of vision with pathological changes.

GC-MS Based Metabolomics Analysis

A 7890B GC system and 7000C mass spectrometer (Agilent Technologies, USA) equipped with an HP-5MS fused silica capillary column was used for metabolomics analysis. We injected 1-μL samples into the GC-MS apparatus with a split ratio of 50:1. Helium was used as the carrier gas with a flow rate at 1 mL/min. The injection temperature was set to 280 °C, the transfer line temperature was 250 °C, and the ion source temperature 230 °C. We set the electron collision ionization to −70 EV and the frequency of acquisition at 20 spectra/s. MS was performed via electrospray ionization with a mass/charge (m/z) full scan range of 50–800.

Data Processing and Multivariate Analysis

We used Agilent Mass Hunter (Version B.07.00, Agilent Technologies, CA, USA) to analyze the raw data from the GC-MS runs. The preprocessing included alignment, retention time correction, baseline filtration, and deconvolution. For metabolite identification, we established a library containing all QC samples, and we applied the US National Institute of Standards and Technology (NIST 14) GC-MS library to identify the unknown metabolites in the QC samples. We considered all metabolites with similarity > 80% as structurally identified. We manually validated all metabolite identifications to reduce deconvolution errors during automated data-processing and to eliminate false identifications. Subsequently, we constructed and used a new spectrum library named "New Library", to match the spectra of the metabolites in the experimental samples.

We obtained an integrated data matrix composed of the peak index (RT-m/z pair), sample name, and corresponding peak area. After peak area normalization using Microsoft Excel™ (Microsoft, Redmond, WA, USA), we used SIMCA-P 14.0 (Umetrics, Sartorius Stedim Biotech) to further analyze the data applying a multivariate analysis including a principal component analysis (PCA) and an orthogonal partial least squares discrimination analysis (OPLS-DA). We performed the comparisons between the two groups using two-tailed Student's *t*-tests. We considered compounds with variable importance in projection (VIP) values > 1.0 and two-tailed Student's *t*-test *p* values < 0.05 as potential differentially-expressed metabolites; we then generated heatmap clusters and pathway analyses entering those identified metabolites into the MetaboAnalyst 5.0 (http://www.metaboanalyst.ca) software.

16S rRNA Sequencing of Gut Microbiota

We performed 16S rRNA gene sequencing analyses using Majorbio Bio-Pharm Technology (Shanghai, China). The microbial genomic DNA was extracted from the colonic contents using an E.Z.N.A.® soil DNA Kit (Omega Bio-tek, Norcross, GA, U.S.), and we separated its fragments by 1% agarose gel electrophoresis. The V3–V4 hyper-variable regions of the bacterial 16S rRNA gene were amplified by TransStart Fastpfu DNA Polymerase (TransGen AP221-02) on a PCR system (Gene Amp 9700, ABI, USA). Subsequently, we extracted the PCR products, purified, and sequenced them using a TruSeqTM DNA Sample Prep Kit (Illumina, USA) on an Illumina MiSeq platform (Illumina, USA). Raw data were obtained according to the RS_ReadsOfinsert1 protocol. We used a QIIME package (Version 1.9.1, http://qiime.org/install/index.html) to obtain high-quality sequences and UPARSE (version 7.1) for operational taxonomic units (OTUs) cluster analysis with a 97% similarity cutoff; chimeric sequences were identified and removed. The Ribosomal Database Program classifier Bayesian algorithm was applied to conduct species taxonomic analyses against the Silva 16S rRNA database using a confidence threshold of 70%, followed by alpha diversity and beta diversity analyses, and the community composition analysis. We used a Phylogenetic Investigation of Communities by Reconstruction of Unobserved States (PICRUSt) 2 (version 1.1.0 http://picrust.github.io/picrust/) for COG function predictions. To assess possible correlations between gut microbiota components and hepatic metabolites, we generated a Spearman correlation heatmap.

Results

MTX-Induced Hepatoxicity in a Mouse Model

ALT and AST levels were significantly higher in the MTX-treated mice than in the control mice (Figure 1A and B, $p < 0.001$). The control group histologic sections showed normal hepatocyte morphology without observed alterations (Figure 1C). However, the liver histologic sections of the challenge group (Figure 1D) had hepatocytes with unevenly colored cytoplasms and nucleoli aggregations in the nuclei. Some hepatocytes were swollen and the cytoplasm was loose and slightly stained. We also observed connective tissue hyperplasia and inflammatory cell infiltrations. There results indicate that MTX caused hepatoxicity in our model mice.

Hepatic Metabolomic Profiles of MTX-Challenged Mice by GC-MS

To determine the effect of MTX on hepatic metabolomic profiles, we applied a GC-MS-based untargeted metabolomics approach in this study. Figure 2A–C depicts the total ion chromatograms (TICs) of the QC, control, and MTX samples of the liver based on GC–MS analyses. The results of our PCA and the OPLS-DA models showed clear differences between the control and the MTX groups (Figure 3A and B). In addition, the parameters obtained through the permutation of 200 tests indicated that the OPLS-DA models and the predication were reliable ($R^2Y = 1.0$, $Q^2Y = 0.959$) (Figure 3C).

We considered metabolites with VIP > 1 from OPLS-DA and p values < 0.05 from Student's t-tests as potential biomarkers responsible for the differences between the two groups. The differentially-expressed metabolites are shown in Table 1, and the cluster analysis of differentially-expressed metabolites of the control group and MTX group are displayed in Figure 3D, which shows that the expressions of uridine and 1-monopalmitin (MG(16:0/0:0/0:0)) were upregulated, while those of various amino acids, D-lactic acid, malic acid, N-dodecane, ethanolamine, glycerol, uracil, and glycerol monostearate (MG(0:0/18:0/0:0)) were downregulated after MTX treatment. Furthermore, the differentially-expressed metabolites were subjected to pathway analysis, and the pathway analysis unveiled that MTX treatment affected amino acids metabolism or biosynthesis; aminoacyl-tRNA biosynthesis; pantothenate, and CoA biosyntheses; glutathione metabolism; porphyrin, and chlorophyll metabolism; and glyoxylate, and dicarboxylate metabolism (Table 2, and Figure 3E and F).

MTX-Induced Gut Microbiota Changes

We used high-throughput 16S RNA sequencing analysis to survey the gut microbiota populations and identify MTX-induced changes. Figure 4A and B shows that community richness and diversity were altered after the MTX challenge (alpha-diversity indices Chao1 and Ace). The Good's coverage index representing the sample coverage detected

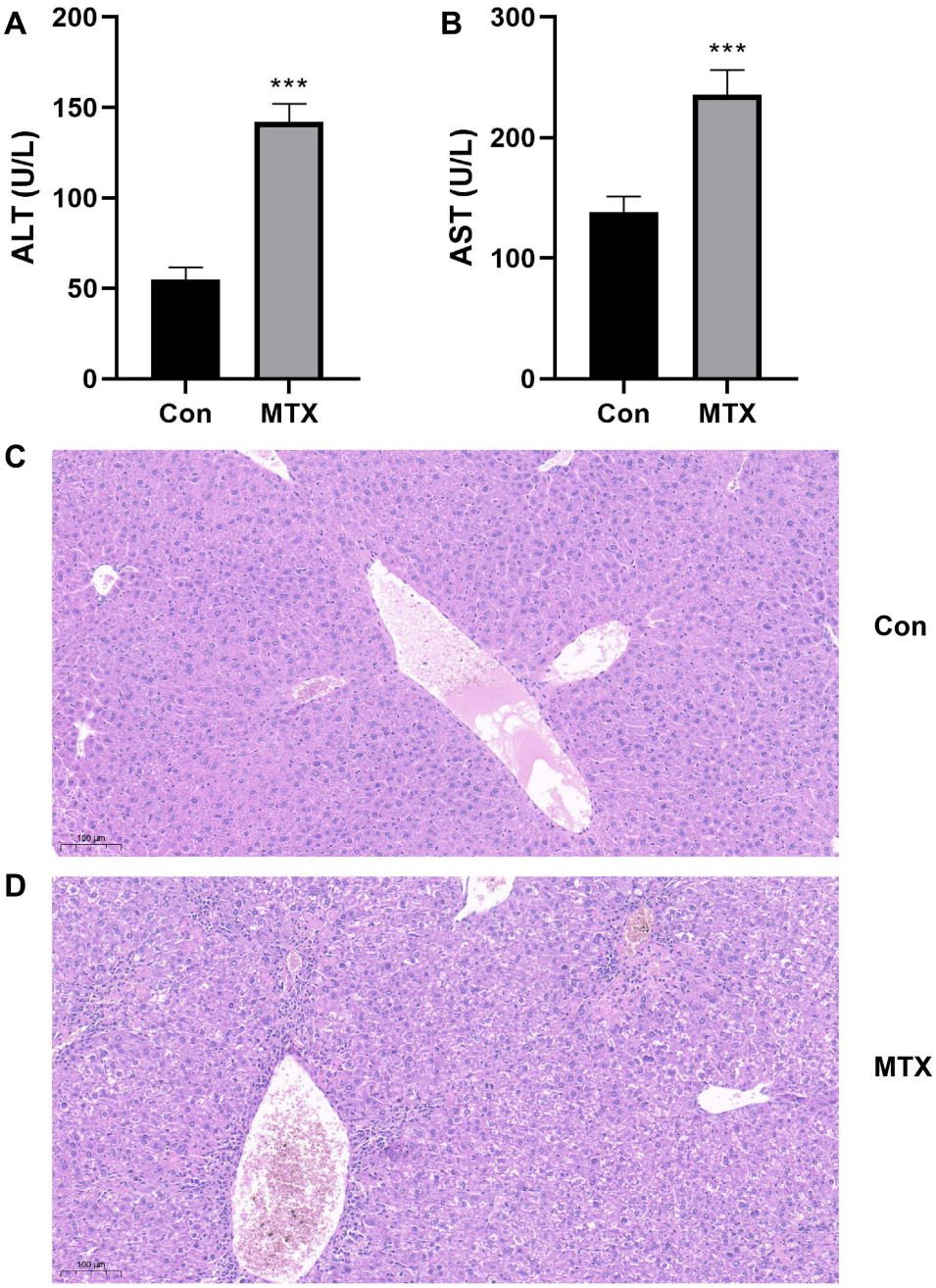

Figure 1 MTX-induced hepatoxicity in a mouse model. (**A**) ALT and (**B**) AST serum levels of challenged and control mice. H&E staining images showing histopathological features of (**C**) control and (**D**) MTX mice. ***$p < 0.001$, compared with control group.

indicated that the sequencing depth was representative of the gut microbiome (Figure 4C). Beta-diversity was analyzed using the principal coordinate analysis (PCoA) (Bray-Curtis distance), and the PCoA on OTU level displayed a significant separation between the control and the MTX groups (Figure 4D).

The community barplot analysis showed that at the phylum level the *Firmicutes* (80.11%), *Actinobacteriota* (8.58%), *Bacteroidota* (6.84%), *Verrucomicrobiota* (3.47%), and *Proteobacteria* (0.08%) were major components of the gut microbiota in the control group; while the same abundances of *Firmicutes* (83.02%), *Actinobacteriota* (13.00%), and *Proteobacteria* (2.69%) were increased but those of *Bacteroidota* (0.78%) and *Verrucomicrobiota* (0.00%) were decreased in the MTX group (Figure 4E). At the genus level, the gut microbiota before the MTX challenge was mainly composed of *Lactobacillus* (15.14%), *Allobaculum* (9.62%), *Ruminococcus* (9.10%), *Dubosiella* (6.26%),

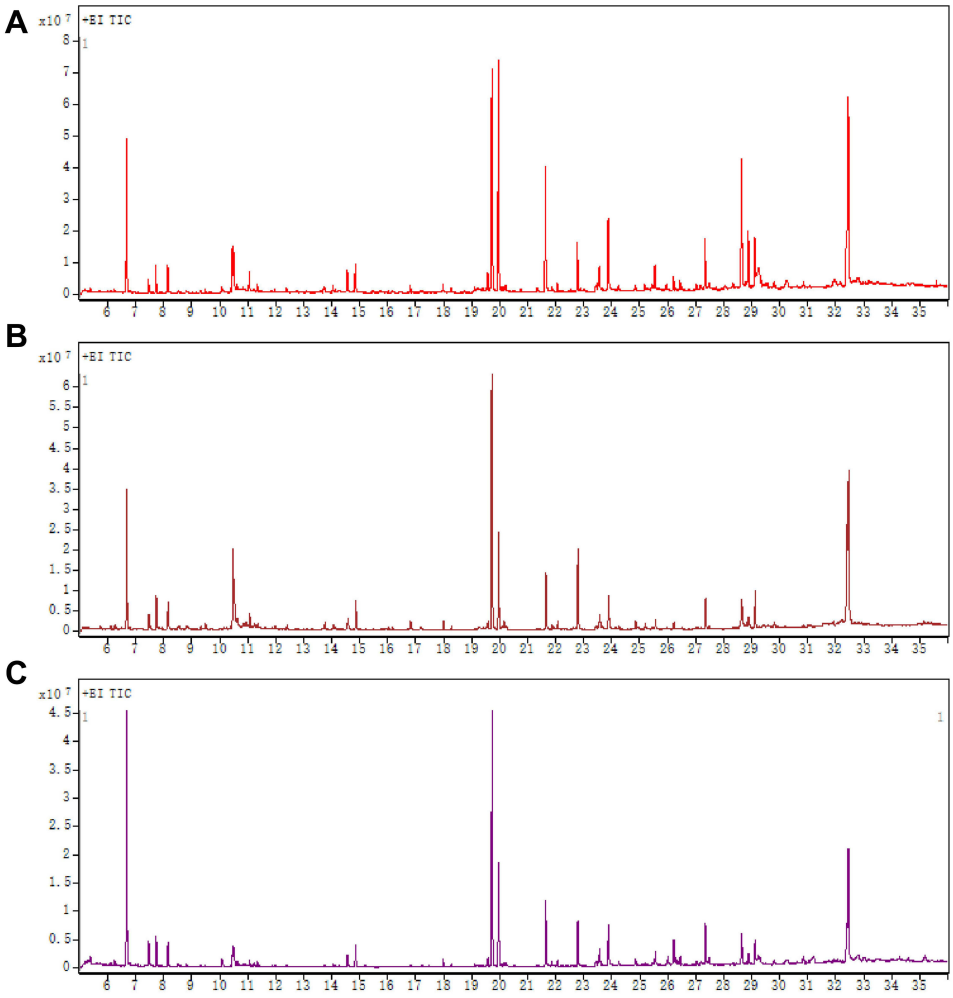

Figure 2 Representative GC-MS TICs of (**A**) QC samples, (**B**) control sample, and (**C**) MTX sample of mice.

norank_f_Muribaculaceae (5.73%), *Blautia* (5.35%), *Enterorhabdus* (3.84%), *Ruminococcus_torques_group* (1.68%), and *Enterococcus* (0.01%); and after the challenge, the abundances of *Blautia* (18.32%), *Ruminococcu_torques_group* (15.63%), *Staphylococcus* (9.83%), *Enterorhabdus* (5.55%), and *Enterococcus* (5.54%) increased, while those of *Lactobacillus* (0.14%), *Allobaculum* (3.16%), *norank_f_Muribaculaceae* (0.31%), *Dubosiella* (1.12%), and *Ruminococcus* (0.07%) decreased (Figure 4F). The clusters of orthologous groups (COG) function classification (Figure 4G) showed that the abundances of energy production and conversion, amino acid transport and metabolism, carbohydrate transport and metabolism, transcription, coenzyme transport and metabolism, and inorganic ion transport and metabolism functions were represented at higher levels in the MTX group than in the control group.

Gut Microbiota Species Population Comparisons

Figure 5A shows the calculated *Firmicutes*/*Bacteroidota* (F/B) ratio, and we found the ratio to be significantly increased in the MTX (106.64) than in the control (11.72) group. We analyzed statistically significant differences in species populations between the control and MTX groups using the Wilcoxon rank-sum test. Figure 5B shows that, at the phylum level, mice in the MTX group had lower amounts of *Bacteroidota* ($p < 0.01$), *unclassified_k_norank_d_Bacteria* ($p < 0.01$), and *Fusobacteriota* ($p < 0.05$), but higher amounts of *Deferribacterota* than those in the control group ($p < 0.05$). At the genus level, the abundances of *Lactobacillus* ($p < 0.01$), *Ruminococcus* ($p < 0.01$), *norank_f_Muribaculaceae* ($p < 0.01$), *unclassified_f_Lachnospiraceae* ($p < 0.05$), *norank_f_Lachnospiraceae* ($p < 0.05$), A2 ($p < 0.01$), *Eubacterium_xylanophilum*_group ($p < 0.05$),

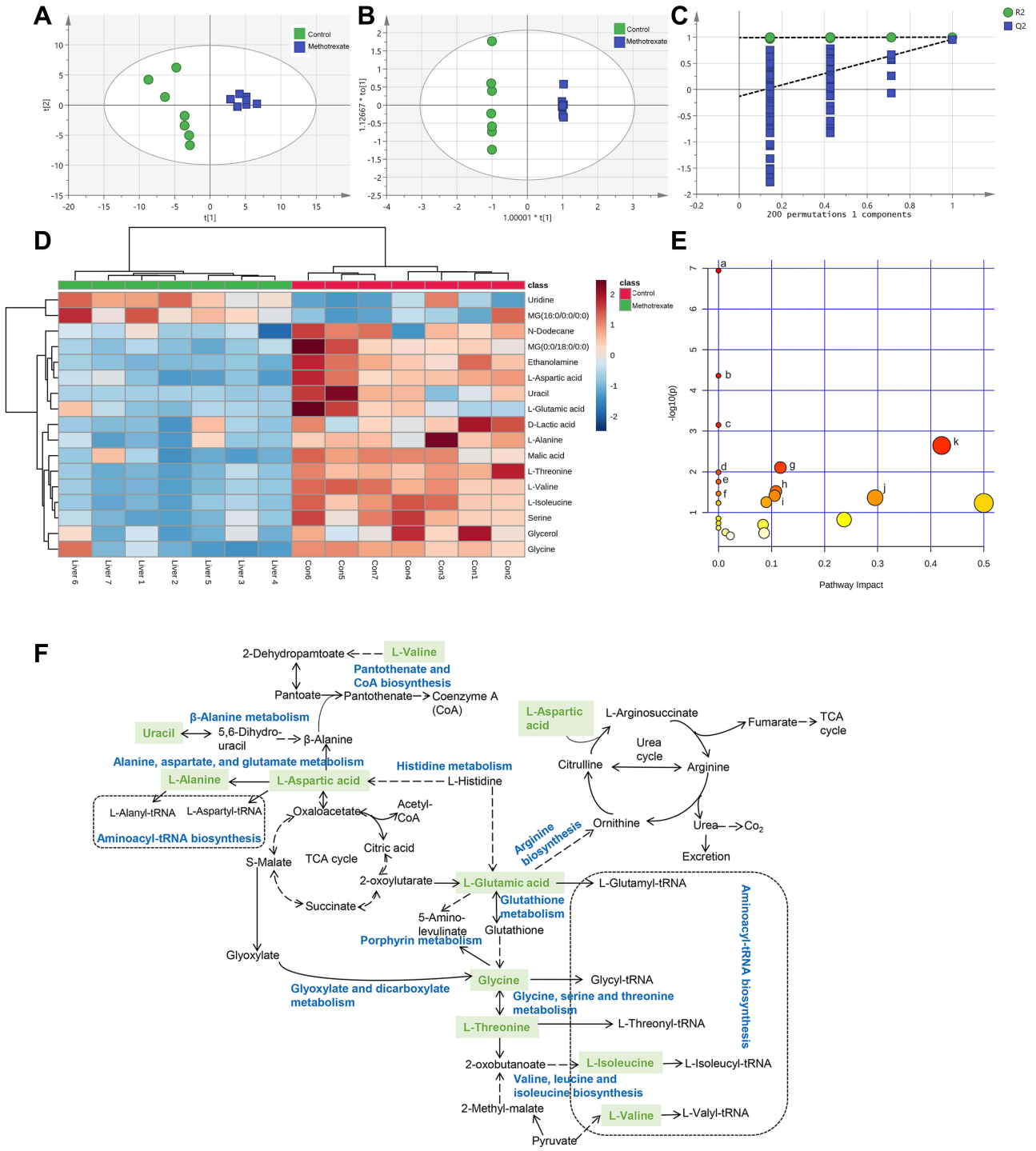

Figure 3 MTX-induced hepatic metabolomic profiles in mice. (**A**) PCA score plot of the control and MTX groups. (**B**) OPLS-DA score plot of control and MTX groups (R^2Y = 1.0, and Q^2Y = 0.959). (**C**) 200 permutation tests of OPLS-DA model. (**D**) Heatmap of relative abundance of differentially-expressed metabolites (VIP > 1.0, and p < 0.05). (**E**) Overview of metabolic pathways affected by MTX (p < 0.05); a, aminoacyl-tRNA biosynthesis; b, valine, leucine and isoleucine biosynthesis; c, pantothenate and CoA biosynthesis; d, histidine metabolism; e, beta-Alanine metabolism; f, porphyrin and chlorophyll metabolism; g, arginine biosynthesis; h, glutathione metabolism; i, glyoxylate and dicarboxylate metabolism; j, glycine, serine and threonine metabolism; k, alanine, aspartate and glutamate metabolism. (**F**) Diagram of the relevant hepatic metabolic pathways affected by MTX. Words in green represent downregulated metabolites in the MTX group mice.

https://doi.org/10.2147/DDDT.S381667 DovePress

Table 1 Differentially-Expressed Metabolites in the Liver of Mice After MTX Challenge

Metabolites	HMDB	KEGG	VIP	*p*-value	Fold Change
D-Lactic acid	HMDB0001311	C00256	1.091	0.002	0.537
L-Valine	HMDB0000883	C00183	1.789	0.000	0.231
L-Alanine	HMDB0000161	C00041	1.395	0.001	0.371
N-Dodecane	HMDB0031444	C08374	1.135	0.003	0.476
Ethanolamine	HMDB0000149	C00189	1.764	0.000	0.229
Glycerol	HMDB0000131	C00116	1.122	0.001	0.556
L-Isoleucine	HMDB0000172	C00407	1.776	0.000	0.241
Glycine	HMDB0000123	C00037	1.394	0.004	0.398
Uracil	HMDB0000300	C00106	1.638	0.005	0.163
Serine	HMDB0062263	C00716	1.226	0.004	0.461
L-Threonine	HMDB0000167	C00188	1.503	0.000	0.379
L-Aspartic acid	HMDB0000191	C00049	1.527	0.000	0.350
Malic acid	HMDB0000744	C03668	1.328	0.001	0.455
L-Glutamic acid	HMDB0000148	C00025	1.242	0.012	0.375
Uridine	HMDB0000296	C00299	1.157	0.002	2.159
MG (16:0/0:0/0:0)	HMDB0011564	-	1.266	0.003	2.637
MG (0:0/18:0/0:0)	HMDB0011535	-	1.575	0.000	0.278

Abbreviations: HMDB, Human Metabolome Database; VIP, variable influence on projection.

Table 2 Pathway Analysis Results Obtained from MetaboAnalyst 5.0

Pathway Name	Raw *p*	-log(*p*)	Impact
Aminoacyl-tRNA biosynthesis	1.14E-07	6.9449	0
Valine, leucine, and isoleucine biosynthesis	4.35E-05	4.3613	0
Pantothenate and CoA biosynthesis	7.05E-04	3.1519	0
Alanine, aspartate, and glutamate metabolism	0.0022573	2.6464	0.42068
Arginine biosynthesis	0.0078672	2.1042	0.11675
Histidine metabolism	0.010255	1.989	0
Beta-Alanine metabolism	0.017438	1.7585	0
Glutathione metabolism	0.03015	1.5207	0.10839
Porphyrin metabolism	0.034301	1.4647	0
Glyoxylate and dicarboxylate metabolism	0.038665	1.4127	0.10582
Glycine, serine, and threonine metabolism	0.043233	1.3642	0.29525

Phascolarctobacterium ($p < 0.05$), *Bifidobacterium* ($p < 0.05$), and *Faecalibaculum* ($p < 0.01$) were significantly reduced in the MTX group mice than in the control mice; but, the amounts of *Staphylococcus* ($p < 0.05$), *Enterococcus* ($p < 0.01$), *Collinsella* ($p < 0.05$), *Streptococcus* ($p < 0.05$), and *Aerococcus* ($p < 0.05$) were remarkably increased in the MTX group mice (Figure 5C).

Relevance Analysis Between Hepatic Metabolic Biomarkers and Gut Microbiota

We assessed genus level associations between gut microbiota and hepatic metabolites by calculating the Spearman correlation coefficient. Our results reveal that some bacteria, including *Phascolarctobacterium, Faecalibaculum, Aerococcus, A2, Streptococcus, norank_f_Muribaculaceae, Enterococcus, Staphylococcus, Collinsella, Ruminococcus*, and *Lactobacillus* present a strong correlation with various metabolites (cor > 0.5 or cor < −0.5). Figure 6 shows that *Phascolarctobacterium, Faecalibaculum, A2, norank_f_Muribaculaceae, Ruminococcus*, and *Lactobacillus* were all positively correlated with metabolites like L-valine, ethanolamine, glycine, serine, L-threonine, and L-aspartic acid; while *Phascolarctobacterium, Faecalibaculum, norank_f_Muribaculacea*e, and *Ruminococcus* were positively correlated with

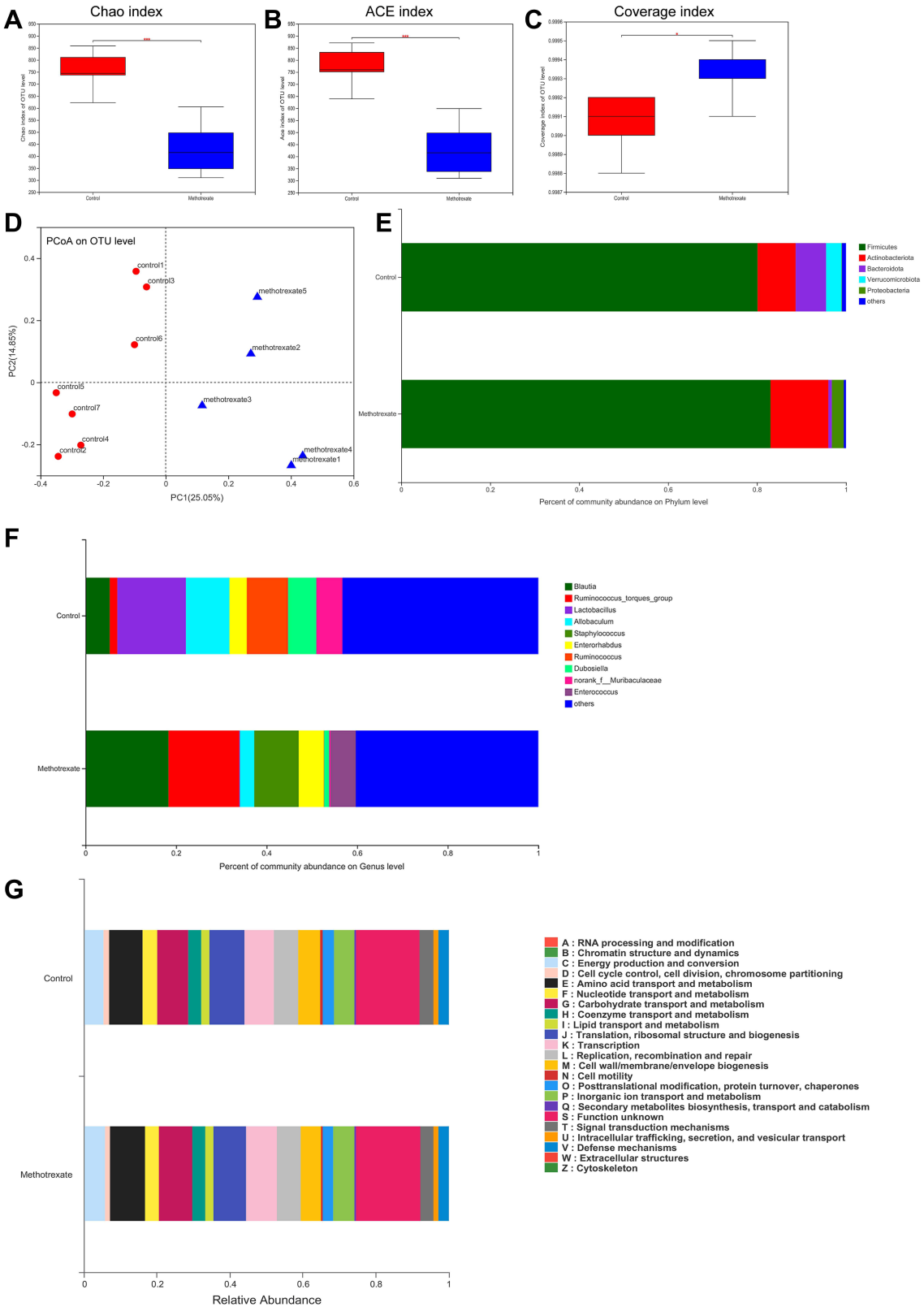

Figure 4 MTX challenge-induced gut microbiota patterns. (**A**–**C**) Alpha-diversity was investigated using the Chao1, Ace, and Good's coverage indexes. (**D**) PCoA score plot on OTU level. Community abundance percentages at the (**E**) phylum or (**F**) genus levels. (**G**) Abundances of PICRUSt-inferred COG function classification in the control and MTX groups. *$p < 0.05$ and ***$p < 0.001$, compared with control group.

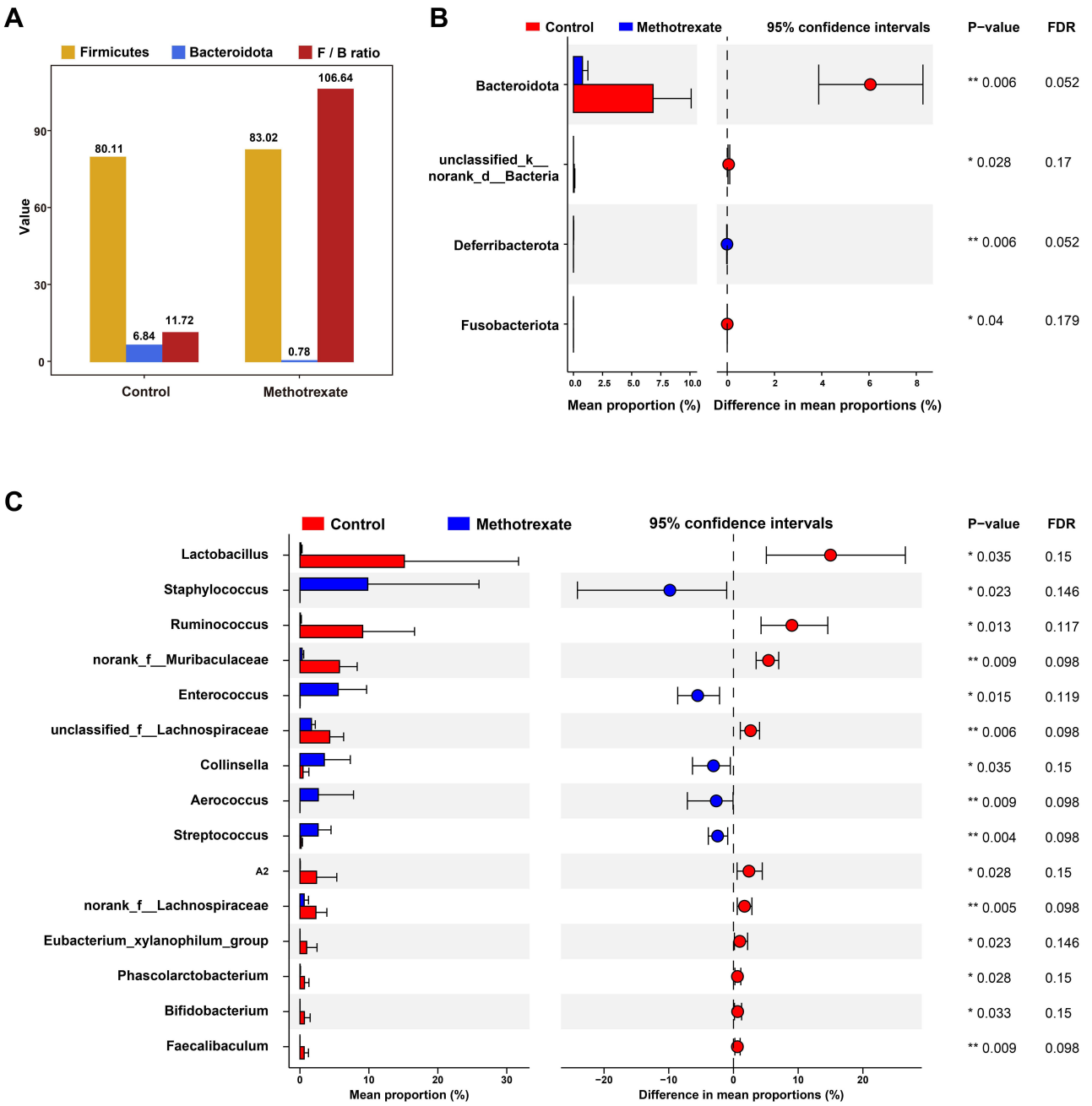

Figure 5 (**A**) F/B ratio of control and MTX mice samples. Wilcoxon rank-sum test bar plot for differences in species populations at the (**B**) phylum and (**C**) genus levels. **p* < 0.05 and ***p* < 0.01 represent statistically significant differences between the control and MTX groups.

uracil but negatively correlated with uridine. In addition, *A2, norank_f_Muribaculaceae*, and *Lactobacillus* were all positively correlated with L-alanine and L-glutamic acid. In addition, *Lactobacillus* showed a positive correlation with D-lactic acid.

Our results also show that *Streptococcus, Enterococcus, Staphylococcus*, and *Collinsella* had a strong negative correlation with metabolites like L-valine, ethanolamine, glycerol, L-isoleucine, glycine, serine, L-threonine, L-aspartic acid, and malic acid, whereas *Streptococcus, Enterococcus*, and *Collinsella* were positively correlated with uridine. Moreover, *Aerococcus, Streptococcus*, and *Staphylococcus* were negatively correlated with D-lactic acid, L-alanine, and L-glutamic acid.

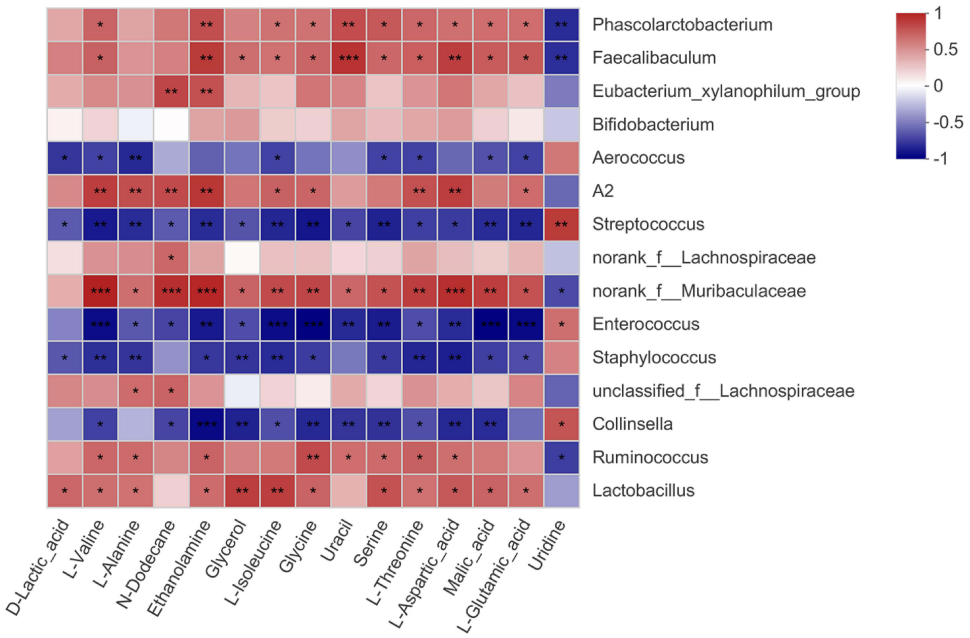

Figure 6 Spearman correlation heatmap of hepatic metabolites and gut microbiota at the genus level. Red squares represent positive correlations, blue squares represent negative correlations, and white squares represent absence of correlations. *$p < 0.05$, **$p < 0.01$, ***$p < 0.001$.

Discussion

Drug-induced liver injury (DILI) is an adverse reaction that can be predicted in patients exposed to toxic doses of specific compounds, but it can also occur unpredictably after application of many common drugs. DILI has become an important cause of acute hepatitis and acute or chronic liver failure.[18] Individuals susceptible to drug-induced adverse reactions may display an altered hepatic metabolism and altered DILI-causative agent excretion, resulting in hepatocyte stress, death, and an activated immune response.[19] Gut microbiome composition changes promoted by drug metabolites can influence the susceptibility to DILI or the innate immune system response by causing enterohepatic circulation changes.[19] DILI models, such as carbon tetrachloride-induced cirrhosis, diethylnitrosamine-induced hepatocellular carcinoma, and acetaminophen-induced hepatotoxicity have been shown to produce changes in the gut microbiome that are essential to the pathophysiological changes observed along the gut-liver axis.[20] Although it has been established that MTX administration can cause hepatotoxicity,[21] the potential association between gut microbiome changes and the hepatic metabolic alterations influenced by MTX remains unclear.

The *Firmicutes* phyla is a major component of the gut microbiota. Increased abundances of *Firmicutes, Actinobacteriota, Verrucomicrobiota, Proteobacteria*, and *Desulfobacterota*, and decreased abundances of *Bacteroidota* and *Campilobacterota* have been associated with the presence of alcoholic liver disease; moreover, the *Firmicutes*/*Bacteroidetes* ratio is significantly decreased after triadica cochinchinensis honey treatment.[22] In addition, the abundance of *Firmicutes* was significantly decreased and the abundance of *Bacteroidota* was increased in a study of mice with acute liver failure.[23] These diverse results indicate that the liver injury caused by different approaches may be associated with different changes in gut microbiota components. Our results show that MTX treatment induced increased abundances of *Firmicutes, Actinobacteriota*, and *Proteobacteria*, but a significant reduction in the abundance of *Bacteroidota*. We confirmed that the F/B ratio was increased after MTX treatment. Our results lend credence to a published finding suggesting that hepatoxicity in Bisphenol A-induced rats was associated with an increased F/B ratio.[24] Moreover, in our MTX-challenged mice, the liver damage indicators (AST and ALT) were increased and H&E staining showed inflammatory cell infiltration indicating that the MTX challenge resulted in both hepatoxicity and gut microbiota components changes. At the genus level, *Faecalibaculum* is representative of the gut microbiota in alcoholic liver injury, and *norank_f_Muribaculaceae, Lactobacillus, unclassified_f_Lachnospiraceae*, and *norank_f_Lachnospiraceae* have been closely associated with alcoholic liver injury.[25] The genera *Aerococcus, Enterococcus, Collinsella*, and *Streptococcus*

have been the predominant proinflammatory bacteria in other diseases,[26,27] and we found that MTX enhanced the abundances of *Aerococcus, Enterococcus, Collinsella*, and *Streptococcus*, implying that MTX might exert proinflammatory effects on the liver. These findings are corroborated by the previous results indicating that MTX can be metabolized into MTX-polyglutamate (MTX-PG) in the body, which gets accumulated intracellularly and provokes hepatocyte oxidative stress, apoptosis, and/or inflammation.[28] Liver inflammation leads to excessive oxygen free radicals and hepatocyte injury. Several intracellular transduction signals depend on normal protein structure and function, and peroxide substances can cause amino acid oxidations that change the activity and antigenicity of enzymes.[29]

The liver plays a critical role in the homeostasis of most amino acids and determines whether specific amino acids are absorbed by the liver or circulated throughout the body. Hepatic amino acids serve as metabolic substrates for a variety of essential compounds.[30] Disrupted amino acid metabolism has been associated with the progression of hepatotoxicity.[31] Three classical hepatotoxin-induced (acetaminophen, bromobenzene, and carbon tetrachloride) acute liver toxicity models showed altered metabolism of different amino acids (glycine, serine and threonine; cysteine and methionine; arginine and proline; glutathione; and alanine, aspartate and glutamate pathways were consistently upregulated).[31] Our findings demonstrate that the decreased abundances of the genera *Phascolarctobacterium, Faecalibaculum, A2, Streptococcus, norank_f_Muribaculaceae, Ruminococcus*, and *Lactobacillus* after the MTX challenge were positively correlated with the presence of various amino acids, but that the abundances of *Staphylococcus, Aerococcus, Enterococcus, Collinsella*, and *Streptococcus* were negatively correlated with the presence of amino acids, indicating that the MTX-induced gut microbiota changes in our mice may have influenced the associated hepatic amino acids metabolism pathway changes known to be present during hepatocyte oxidative stress, apoptosis, or inflammation (changes in biosynthetic pathways of valine, leucine, and isoleucine; and arginine; and in the metabolic pathways of alanine, aspartate, and glutamate; histidine; and glycine, serine, and threonine).[29]

The tRNA-charged amino acids are direct precursors of protein synthesis, and the number and distribution of amino acids in the aminoacyl-tRNA pool might be strongly associated with the protein synthesis rate in tissues.[32] Fine particulate matter exposure was shown to result in liver toxicity and further metabolic analysis confirmed that aminoacyl-tRNA biosynthesis as well as other amino acid metabolism pathways were significantly affected.[33] After alcohol intake, different metabolic pathways including aminoacyl-tRNA biosynthesis; alanine, aspartate, and glutamate metabolism; and energy metabolism have been shown to be altered.[34] In this study, we found various amino acids enriched in the aminoacyl-tRNA biosynthesis pathway such as glycine, L-aspartic acid, L-valine, L-alanine, L-isoleucine, L-threonine, L-glutamic acid, and others downregulated in the MTX group mice, indicating that protein synthesis was disrupted after the MTX challenge. In addition, we found the genera *Phascolarctobacterium, Faecalibaculum, A2, Streptococcus, norank_f_Muribaculaceae, Ruminococcus*, and *Lactobacillus* to be positively correlated with aminoacyl-tRNA biosynthesis, and *Staphylococcus, Aerococcus, Enterococcus, Collinsella*, and *Streptococcus* to be negatively correlated with aminoacyl-tRNA biosynthesis in the liver. We also found altered metabolic pathways other than that of aminoacyl-tRNA biosynthesis including amino acid metabolic pathways (biosyntheses of valine, leucine, and isoleucine; and arginine; and, metabolism of alanine, aspartate, and glutamate; histidine; beta-alanine; and glycine, serine, and threonine); biosyntheses of pantothenate, and CoA; and, metabolic pathways of energy (glyoxylate, dicarboxylate); and biosyntheses of pantothenate, and CoA. These results were consistent with our COG function prediction, which showed that MTX influenced energy production and conversion, amino acid transport and metabolism, and carbohydrate transport and metabolism.

Glutamic acid is a versatile amino acid that can be found in the central nervous system and other organs. Under physiological conditions, glutamic acid is a crucial hepatic amino acid metabolite produced by transdeamination during the catabolism of arginine, ornithine, proline, histidine, and glutamine.[35] Efflux of glutamic acid from hepatocytes largely determines the glutamic acid level in vivo.[36] We speculated that liver dysfunction might enhance glutamic acid efflux and disrupt amino acid metabolism, resulting in decreased levels of hepatic glutamic acid and other amino acids after MTX challenge. In the intestine, host and microbes metabolize endogenous (bile acids, amino acids) as well as exogenous (from diet and environmental exposure) substrates, the products of which translocate to the liver through the portal vein and influence the liver functions.[10] Alterations in glutamine metabolism have been found in the liver of mice after CCl_4-induced acute liver injury, and those findings indicate that glutamine metabolism has a pivotal role in the regulation of proliferation and activation of hepatic stellate cells, which might partly explain the effect of glutamic acid on hepatocyte proliferation.[37] In a lipopolysaccharide (LPS)-caused liver injury model, the hepatic glutamic acid

content was apparently decreased, whereas α-ketoglutarate (AKG) supplementation promoted the accumulation of glutamic acid in the liver; suggesting that AKG application attenuated LPS-induced liver injury through inhibition of the oxidative capacity and promotion of energy metabolism.[38] In this study, we found downregulated L-glutamic acid in several amino acid metabolic pathways (including those of alanine, aspartate, and glutamate; histidine; and glutathione; and arginine biosynthesis) which suggests that L-glutamic acid is implicated in hepatocyte proliferation and energy metabolism through its regulation of various amino acid metabolic pathways, not as a neurotransmitter. 16S RNA analysis results showed that *Phascolarctobacterium, Faecalibaculum, A2, norank_f_Muribaculaceae*, and *Lactobacillus* were all positively correlated with L-glutamic acid, while *Aerococcus, Streptococcus, Enterococcus*, and *Staphylococcus* were negatively correlated with it, indicating that these genera are potentially associated with the L-glutamic acid-related hepatocyte proliferation and energy metabolism pathways. Our COG function classification also confirmed that energy production and conversion, and amino acid transport and metabolism were enhanced in the gut of MTX-treated mice.

Interestingly, our metabolomics analysis and COG function prediction both identified MTX-induced liver toxicity as being associated with CoA biological processes. In our study, L-aspartic acid, L-valine, and uracil were all decreased after the MTX challenge, implying that pantothenate and CoA biosyntheses were dysregulated in the liver. According to the KEGG pathway analysis (https://www.kegg.jp/pathway/map00770), L-valine and L-aspartic acid can be hydrolyzed and converted to pantothenate through multiple processes. Moreover, pantothenate is catalyzed by kinase and further metabolized to CoA. Pantothenate (also known as vitamin B5) is the precursor for CoA essential for 4% of all known enzymatic reactions in vivo.[39] Mangiferin calcium salt has been found to attenuate type 2 diabetes and non-alcoholic fatty liver, while affecting the biosyntheses of pantothenate, and CoA; fatty acid, citric acid cycle precursors; and arginine; and the tryptophan metabolic pathway.[40] However, MTX's effects on the pantothenate and CoA biosynthesis pathway remain unclear. COG function prediction identified increased abundances of coenzyme transport and metabolism, suggesting that MTX might promote the transport and metabolism of coenzymes. The amounts of *Streptococcus, Enterococcus*, and *Collinsella* were increased in MTX group mice, and their presence was negatively correlated with hepatic L-aspartic acid, L-valine, and uracil, suggesting that *Streptococcus, Enterococcus*, and *Collinsella* might be implicated in coenzyme transport and metabolism.

Our main focus was the preliminary assessment of potential MTX-induced hepatotoxicity mechanisms, and we found correlations between differential gut microbiota and hepatic metabolites; however, identifying hub microbiota and metabolites remains important. Fecal bacteria transplantation experiments should be conducted to validate our results.

Conclusion

MTX exposure led to hepatoxicity associated with gut microbiota and metabolomic pathways changes. MTX disrupted mainly the biosyntheses of aminoacyl-tRNA; and, pantothenate, and CoA; and, the metabolic pathways of amino acids; energy; porphyrin, and chlorophyll; and glutathione. In addition, MTX increased the abundances of *Staphylococcus, Enterococcus, Collinsella, Streptococcus*, and *Aerococcus*, and decreased the abundances of *Lactobacillus, Ruminococcus, norank_f_Muribaculaceae, unclassified_f_Lachnospiraceae, norank_f_Lachnospiraceae, A2, Eubacterium_xylanophilum_group, Phascolarctobacterium, Bifidobacterium*, and *Faecalibaculum*. Correlation analyses provide a promising approach to fully understand MTX-induced hepatoxicity.

Funding

This study was supported by the Jining Key Research and Development Program (2021YXNS042), and the Doctoral Research Startup Foundation of Jining First People's Hospital (No. 2019003).

Disclosure

The authors report no conflicts of interest in this work.

References

1. Koźmiński P, Halik PK, Chesori R, Gniazdowska E. Overview of dual-acting drug methotrexate in different neurological diseases, autoimmune pathologies and cancers. *Int J Mol Sci*. 2020;21(10):3483. doi:10.3390/ijms21103483
2. Hannoodee M, Mittal M. Methotrexate. In: *StatPearls*. StatPearls Publishing; 2021.
3. Solomon DH, Glynn RJ, Karlson EW, et al. Adverse effects of low-dose methotrexate: a randomized trial. *Ann Intern Med*. 2020;172(6):369–380. doi:10.7326/M19-3369
4. Bath RK, Brar NK, Forouhar FA, Wu GY. A review of methotrexate-associated hepatotoxicity. *J Dig Dis*. 2014;15(10):517–524. doi:10.1111/1751-2980.12184
5. Visser K. Van der Heijde D. Risk and management of liver toxicity during methotrexate treatment in rheumatoid and psoriatic arthritis: a systematic review of the literature. *DARE*. 2009;27(6):1017–1025.
6. Yang T, Richards EM, Pepine CJ, Raizada MK. The gut microbiota and the brain–gut–kidney axis in hypertension and chronic kidney disease. *Nat Rev Nephrol*. 2018;14(7):442–456. doi:10.1038/s41581-018-0018-2
7. Lässiger-Herfurth A, Pontarollo G, Grill A, Reinhardt C. The gut microbiota in cardiovascular disease and arterial thrombosis. *Microorganisms*. 2019;7(12):691. doi:10.3390/microorganisms7120691
8. Lu L, Chen X, Liu Y, Yu X. Gut microbiota and bone metabolism. *FASEB J*. 2021;35(7):e21740. doi:10.1096/fj.202100451R
9. Tilg H, Cani PD, Mayer EA. Gut microbiome and liver diseases. *Gut*. 2016;65(12):2035–2044. doi:10.1136/gutjnl-2016-312729
10. Tripathi A, Debelius J, Brenner DA, et al. The gut–liver axis and the intersection with the microbiome. *Nat Rev Gastroenterol Hepatol*. 2018;15(7):397–411.
11. Yi Z, Liu X, Liang L, et al. Antrodin A from Antrodia camphorata modulates the gut microbiome and hepatic metabolome in mice exposed to acute alcohol intake. *Food Funct*. 2021;12(7):2925–2937. doi:10.1039/D0FO03345F
12. Roghani M, Kalantari H, Khodayar MJ, et al. Alleviation of liver dysfunction, oxidative stress and inflammation underlies the protective effect of ferulic acid in methotrexate-induced hepatotoxicity. *Drug Des Devel Ther*. 2020;14:1933. doi:10.2147/DDDT.S237107
13. Loke MF, Chua EG, Gan HM, et al. Metabolomics and 16S rRNA sequencing of human colorectal cancers and adjacent mucosa. *PLoS One*. 2018;13(12):e0208584. doi:10.1371/journal.pone.0208584
14. Peng W, Huang J, Yang J, et al. Integrated 16S rRNA sequencing, metagenomics, and metabolomics to characterize gut microbial composition, function, and fecal metabolic phenotype in non-obese type 2 diabetic Goto-Kakizaki rats. *Front Microbiol*. 2020;10:3141. doi:10.3389/fmicb.2019.03141
15. Liu YJ, Tang B, Wang FC, et al. Parthenolide ameliorates colon inflammation through regulating Treg/Th17 balance in a gut microbiota-dependent manner. *Theranostics*. 2020;10(12):5225. doi:10.7150/thno.43716
16. Forsgård RA, Marrachelli VG, Korpela K, et al. Chemotherapy-induced gastrointestinal toxicity is associated with changes in serum and urine metabolome and fecal microbiota in male Sprague–Dawley rats. *Cancer Chemother Pharmacol*. 2017;80(2):317–332. doi:10.1007/s00280-017-3364-z
17. Freeman-Narrod M, Narrod SA. Chronic toxicity of methotrexate in mice. *J Natl Cancer Inst*. 1977;58(3):735–741. doi:10.1093/jnci/58.3.735
18. Devarbhavi H, Patil M, Reddy VV, Singh R, Joseph T, Ganga D. Drug-induced acute liver failure in children and adults: results of a single-centre study of 128 patients. *Liver Int*. 2018;38(7):1322–1329. doi:10.1111/liv.13662
19. Andrade RJ, Chalasani N, Björnsson ES, et al. Drug-induced liver injury. *Nat Rev Dis Primers*. 2019;5(1):1–22. doi:10.1038/s41572-019-0105-0
20. Dey P. The role of gut microbiome in chemical-induced metabolic and toxicological murine disease models. *Life Sci*. 2020;258:118172. doi:10.1016/j.lfs.2020.118172
21. Kim J, Kim Y, Choi J, et al. Recapitulation of methotrexate hepatotoxicity with induced pluripotent stem cell-derived hepatocytes from patients with rheumatoid arthritis. *Stem Cell Res Ther*. 2018;9(1):1–15. doi:10.1186/s13287-018-1100-1
22. Luo L, Zhang J, Liu M, et al. Monofloral triadica cochinchinensis honey polyphenols improve alcohol-induced liver disease by regulating the gut microbiota of mice. *Front Immunol*. 2021;12:673903. doi:10.3389/fimmu.2021.673903
23. Zhao J, Liu L, Xin L, et al. The protective effects of a modified xiaohua funing decoction against acute liver failure in mice induced by D-Gal and LPS. *Evid Based Complementary Altern Med*. 2022;2022:6611563. doi:10.1155/2022/6611563
24. Liu RJ, Liu BP, Tian LM, et al. Exposure to bisphenol A caused hepatoxicity and intestinal flora disorder in rats. *Int J Mol Sci*. 2022;23(14):8042. doi:10.3390/ijms23148042
25. Zhou J, Zhang N, Zhao L, et al. Protective effects of honey-processed astragalus on liver injury and gut microbiota in mice induced by chronic alcohol intake. *J Food Qual*. 2022;2022:1–12.
26. Li BY, Xu XY, Gan RY, et al. Targeting gut microbiota for the prevention and management of diabetes mellitus by dietary natural products. *Foods*. 2019;8(10):440. doi:10.3390/foods8100440
27. Martínez JE, Vargas A, Pérez-Sánchez T, Encío IJ, Cabello-Olmo M, Barajas M. Human microbiota network: unveiling potential crosstalk between the different microbiota ecosystems and their role in health and disease. *Nutrients*. 2021;13(9):2905. doi:10.3390/nu13092905
28. Ezhilarasan D. Hepatotoxic potentials of methotrexate: understanding the possible toxicological molecular mechanisms. *Toxicology*. 2021;458:152840. doi:10.1016/j.tox.2021.152840
29. Zhu R, Wang Y, Zhang L, Guo Q. Oxidative stress and liver disease. *Hepatol Res*. 2012;42(8):741–749. doi:10.1111/j.1872-034X.2012.00996.x
30. Paulusma CC, Lamers W, Broer S. van de Graaf SF. Amino acid metabolism, transport and signalling in the liver revisited. *Biochem Pharmacol*. 2022;201:115074. doi:10.1016/j.bcp.2022.115074
31. Pannala VR, Estes SK, Rahim M, et al. Toxicant-induced metabolic alterations in lipid and amino acid pathways are predictive of acute liver toxicity in rats. *Int J Mol Sci*. 2020;21(21):8250. doi:10.3390/ijms21218250
32. Wolfe RR, Song J, Sun J, Zhang XJ. Total aminoacyl-transfer RNA pool is greater in liver than muscle in rabbits. *J Nutr*. 2007;137(11):2333–2338. doi:10.1093/jn/137.11.2333
33. Shi C, Han X, Mao X, Fan C, Jin M. Metabolic profiling of liver tissues in mice after instillation of fine particulate matter. *Sci Total Environ*. 2019;696:133974. doi:10.1016/j.scitotenv.2019.133974

34. Fang H, Zhang AH, Sun H, Yu JB, Wang L, Wang XJ. High-throughput metabolomics screen coupled with multivariate statistical analysis identifies therapeutic targets in alcoholic liver disease rats using liquid chromatography-mass spectrometry. *J Chromatogr B*. 2019;1109:112–120. doi:10.1016/j.jchromb.2019.01.017
35. Brosnan ME, Brosnan JT. Hepatic glutamate metabolism: a tale of 2 hepatocytes. *Am J Clin Nutr*. 2009;90(3):857S–861S. doi:10.3945/ajcn.2009.27462Z
36. Pfennig T, Herrmann B, Bauer T, Schömig E, Gründemann D. Benzoic acid and specific 2-oxo acids activate hepatic efflux of glutamate at OAT2. *Biochim Biophys Acta*. 2013;1828(2):491–498. doi:10.1016/j.bbamem.2012.08.026
37. Li J, Ghazwani M, Liu K, et al. Regulation of hepatic stellate cell proliferation and activation by glutamine metabolism. *PLoS One*. 2017;12(8):e0182679. doi:10.1371/journal.pone.0182679
38. Wang L, Hou Y, Yi D, et al. Dietary supplementation with glutamate precursor α-ketoglutarate attenuates lipopolysaccharide-induced liver injury in young pigs. *Amino Acids*. 2015;47(7):1309–1318. doi:10.1007/s00726-015-1966-5
39. Leonardi R, Zhang YM, Rock CO, Jackowski S. Coenzyme A: back in action. *Prog Lipid Res*. 2005;44(2–3):125–153. doi:10.1016/j.plipres.2005.04.001
40. Lin H, Teng H, Wu W, et al. Pharmacokinetic and metabolomic analyses of Mangiferin calcium salt in rat models of type 2 diabetes and non-alcoholic fatty liver disease. *BMC Pharmacol Toxicol*. 2020;21(1):1–12. doi:10.1186/s40360-020-00438-x